Proceedings of the
International Conference on Mechanical Engineering and Renewable Energy 2013
(ICMERE2013) 1 - 3 May 2014, Chittagong, Bangladesh

ICMERE2013-PI-281

FABRICATION OF NANOPOROUS NICKEL FOAM BY POWDER METALLURGY TECHNIQUE AND CHEMICAL DEALLOYING

Md. Arafat Rahman[1], Xiaojian Wang[2] and Cuie Wen[3,*]

[1-3]Faculty of Engineering and Industrial Science,
Swinburne University of Technology,
Hawthorn, Victoria 3122, Australia

[1]mdarafatrahman@swin.edu.au, [2]xiaojianwang@swin.edu.au, [3,*]cwen@swin.edu.au

Abstract- *Porous metals with a large surface-to-volume ratio, light weight, and excellent electrical/thermal conductivity have attracted much attention. In this study, Ni_x-Al_{1-x} alloys were prepared by mechanical alloying and sintering. Thereafter, porous nickel (Ni) foams were fabricated through chemically de-alloying the aluminum (Al) from the Ni_xAl_{1-x}* alloys using a sodium hydroxide (NaOH) solution. *The phase compounds and microstructure of nanoporous nickel have been investigated using X-ray diffraction (XRD), scanning electron microscopy combined with energy dispersive X-ray analysis (SEM-EDX). SEM images revealed that porous Ni foams with approximately 40nm pore diameter and 100 nm ligament length were obtained from the dealloying of the Ni_x-Al_{1-x} alloys.*

Keywords: Porous materials, Nanoporous, Powder metallurgy, Dealloying.

1. INTRODUCTION

Porous materials only started to be used in engineering applications at the very beginning of the 20th century [1]. Metal foams are a new class of materials and have been used as car body structures, optical systems, biomedical implants and for space applications, light weight conformal pressure tanks, electrodes for batteries, and many other applications in small scale. Nanoporous materials possess many good properties including high surface area, ultra-low density, high strength to weight ratio, and good characteristics of electrical and thermal conductivity [2-5]. In addition, it can be used for catalytic, gas sensing, and mechanical applications [6, 7]. In terms of the description from the International Union of Pure and Applied Chemistry (IUPAC) [8, 9], porous materials can be considered into three types by their pore size: microporous (pore size <2 nm), mesoporous (2 nm < pore size > 50 nm) and macroporous (pore size > 50 nm). In this definition, nanoporous metal foam is a three dimensional structure consisting of interconnected metallic particles or filaments which has not less than 50% porosity. Nanoporous metal foams having these characteristics show the low relative density ($Density_{foam}/Density_{bulk}$), enhanced plasmatic behaviour and high surface area [10].

Nanostructured nickel is a potentially low-cost alternative to precious-metal catalysts [11]. The benefit of employing a nanoporous Ni is an electronic band structure that promotes the reaction of interest and a specific high surface area to maximize reagent contact. The high surface area of porous metals allows the electrolyte to access more of the metal, resulting fast charge/discharge characteristics. However, nickel is typically used as the positive electrode, being one of few materials that can withstand repeated cycling and the associated volumetric changes. Nanoporous nickel foam can be obtained by the alkaline leaching of aluminium from Ni-Al Raney nickel [12], chemical vapour deposition(CVD) [13-15], electrodeposition [16], dealloying [17, 18], powder metallurgy technique [15], and so on. However, these processes were found to be imperfect due to limitations of controlling the pore sizes and relative density which are important for the properties of metallic foams [19, 20]. Dealloying has been selected as the fabrication process for nanoporous nickel in this study, due to numerous merits such as easy handling and simple instrumental setup. The morphology and chemical nature of the as-prepared nanoporous Ni have been characterized using SEM and EDX; crystallinity and phase information were obtained by XRD.

2. EXPERIMENTAL

Ni-Al alloys having composition of $Ni_{50}Al_{50}$, $Ni_{40}Al_{60}$, and $Ni_{30}Al_{70}$ (wt % hereafter) were prepared by powder metallurgy. Elemental Ni and Al powders (both with a purity of 99.7% and particle size 40 μm) were used as starting materials (Australian metal powders suppliers Pty Ltd.). The metal powders with mentioned compositions were ball milled (Retsch PM 400) of 10 h at 200 rpm with 20:1 ball to powder ratio. Thereafter, the mixture was green compacted at 400 MPa and sintered. The sintering was carried in two steps in GERO Vacuum furnace. The first step was performed at 550 ^{O}C holding for 5 h; and the second step was carried out at 1050 ^{O}C and holding for 5 h and rested in furnace cooling. Finally, the sintered Ni_xAl_{1-x} alloys were dealloyed in a handmade cell for 5 h in a 5M NaOH electrolyte at 60 ^{O}C. The procedure is illustrated in Fig. 1.

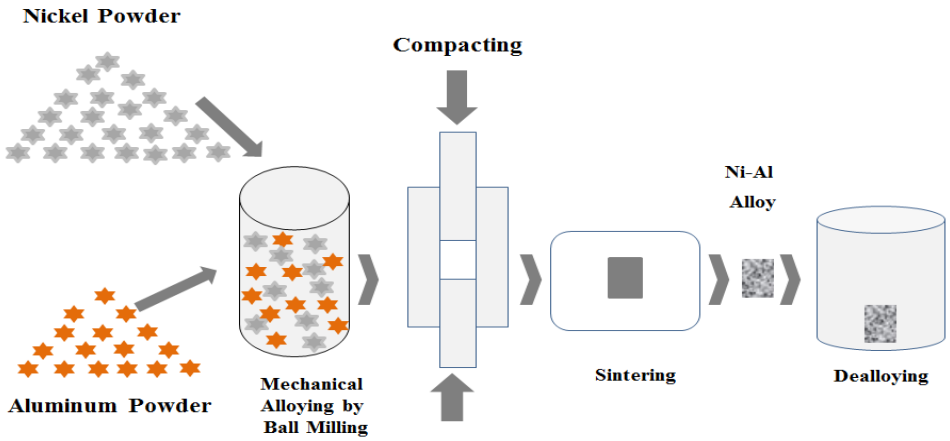

Fig.1: Schematic diagram of the fabrication process of nanoporous nickel foam

The morphologies and chemical compositions of the samples were examined with a scan electron microscope combined with energy-dispersive X-ray spectrometer (SUPRA 40VP, Zeiss).

X-ray diffraction patterns were obtained by using Cu Kα as the radiation source. The diffraction patterns were recorded over a 2θ range from 30 to 60^{o} at a step size of 0.02^{o}.

3. MECHANISM OF DEALLOYING

Dealloying can be interpreted as a reaction-diffusion process, where the less noble metal in a solid solution is dissolved at the solid/liquid interface to an acid or alkaline solution, leaving behind a porous residue.

For dealloying to occur, the two elements of a binary alloy must have sufficient different equilibrium potentials, allowing the active one to dissolve away while the other remains intact [21]. Two important parameters should be considered for the experimental observation on the dealloying. One is the parting time, limiting concentration of the inert component in an alloy. In general, dealloying does not occur above the limiting concentration. The critical potential (E_c) is the other important factor for the dealloying process, marking the transition from alloy passivity planar to the rapid formation of pores [21, 22]. Therefore, dealloying usually refers to selective dissolution at a potential above the critical potential. However, microscopic observations at an atomic-scale by means of scanning tunneling microscopy (STM) have revealed that selective dissolution also occurs bellow E_c, although the dissolution rate is relatively slow [23].

Ni_xAl_{1-x} alloys have been used as starting materials as earlier mentioned. However, aluminum does not react with water under normal circumstances, as an impermeable protective layer composed of aluminum hydroxide either forms within a seconds or is already in place. The formation of a protective layer is prevented with the addition of sodium hydroxide. With the production of aluminates ($Al(OH)_4^-$), the amphoteric (capable of acting as either an acid or a base) aluminum hydroxide $Al(OH)_3$ goes in solution as follows;

$$2\ Al(s) + 6\ H_2O \rightarrow 2Al(OH)_3 + 3H_2(g) \quad (1)$$

$$2Al(OH)_3 + 2NaOH \rightarrow 2Na^+ + 2[Al(OH)_4]^- \quad (2)$$

$$2\ Al(s) + 2NaOH + 6\ H_2O \rightarrow 2Na^+ + 2[Al(OH)_4]^- + 3H_2(g) \quad (3)$$

During these reactions, Al atoms in Ni-Al intermetallic compound are continuously dissolved into the solution and hydrogen (H_2) bubbles come out of the sample surface. The bubble is rapidly emerged at the beginning of the dealloying; it slowly disappears as dealloying is processed. It indicates that the dealloying rate gradually decreases. The reaction practically stops when all Al is dissolved in the NaOH solution. The Ni atoms remained during chemical dealloying stable because of Ni does not react with NaOH.

4. RESULTS AND DISCUSSION

Figure 2 shows the XRD patterns of the sintered samples before dealloying. The patterns confirm the formation of Ni-Al intermetallic phases. The crystallographic parameters of intermetallic phases have been shown in Table 1. The patterns indicate the formation of Al_3Ni and Al_3Ni_2 in the sintered alloys.

However, other intermetallic phases such as Al_2Ni and Al_4Ni_3 have also been formed. Inspection of the XRD spectra (Fig. 2) reveals that the diffraction peaks for the samples with higher Ni composition are broader. The broadening width can be converted to the crystallite thickness by Scherrer's equation as follows;

$$T = K*\lambda/B*\cos(\theta) \quad (4)$$

Where, T = the mean size of the ordered (crystalline) domains, which may be smaller or equal to the grain size, and B= full width at half maximum (FWHM). K= A dimensionless shape factor depends on crystallite shape (0.6 to 0.9), λ= X-ray wavelength (1.5046 A^{o}) and θ= Bragg angle. The XRD pattern of the Ni_xAl_{1-x} exhibits a superimposed of sharp crystal peaks. These crystal peaks match with (131), (230), (122), (110), (112) and (301) crystal planes of Al_3Ni and (012), and (110) crystal planes of Al_3Ni_2, respectively.

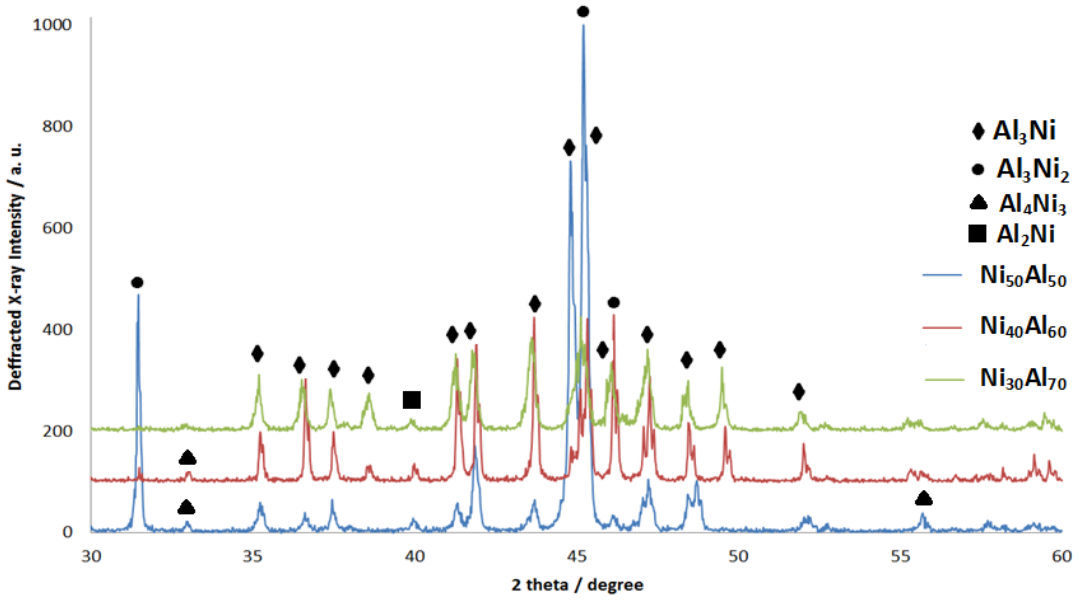

Fig. 2: XRD patterns of Ni_xAl_{1-x} alloys before dealloying

Table 1: Crystallographic parameters of the Ni_xAl_{1-x} alloys

Sample(%wt)	Compound	2θ/deg	Intensity/ a.u	h	k	l	dA°	fwhm(deg)	Crystalline size (nm)
$Ni_{50}Al_{50}$	Al_3Ni	43.643	877	1	3	1	2.0722	0.30	28.72
		45.315	874	2	3	0	1.9996	0.30	28.89
		47.230	650	1	2	2	1.9229	0.50	17.39
	Al_3Ni_2	45.154	999	0	1	2	2.0063	0.20	42.90
		44.876	880	1	1	0	2.0181	0.20	42.86
$Ni_{40}Al_{60}$	Al_3Ni	43.643	877	1	3	1	2.0722	0.20	42.67
		45.315	874	1	1	2	1.9996	0.20	42.92
		47.230	650	1	2	2	1.9229	Unmeasurable	N/A
	Al_3Ni_2	45.250	999	0	1	2	2.0023	0.25	34.14
		44.972	875	1	1	0	2.0140	Unmeasurable	N/A
$Ni_{30}Al_{70}$	Al_3Ni	45.220	921	3	0	1	2.0036	0.40	21.45
		43.552	910	1	3	1	2.0763	Unmeasurable	N/A
		47.133	677	1	2	2	1.9266	0.40	21.61

The crystal size of the $Ni_{50}Al_{50}$ alloy is ranging from 17.39 nm to 42.90nm. In addition, the crystal size of the $Ni_{40}Al_{60}$ alloy is ranging from 34.14 nm to 42.67 nm, whereas the crystal size of $Ni_{30}Al_{70}$ alloy is less than 22 nm which is shown in Fig. 3 (a). The crystal size of the compounds Al_3Ni and Al_3Ni_2 have been reduced with increasing the content of Ni in the alloys as shown in Fig. 3 (b). However, the crystal size of the compound Al_3Ni_2 is larger than the Al_3Ni. Although the phase constitution is the same in the three Ni-Al alloys, the size and amount of the Al_3Ni and Al_3Ni_2 phases are different and depend upon the alloy composition. These compounds had the significant influence on the dealloying process and formation of nanoporous Ni foam.

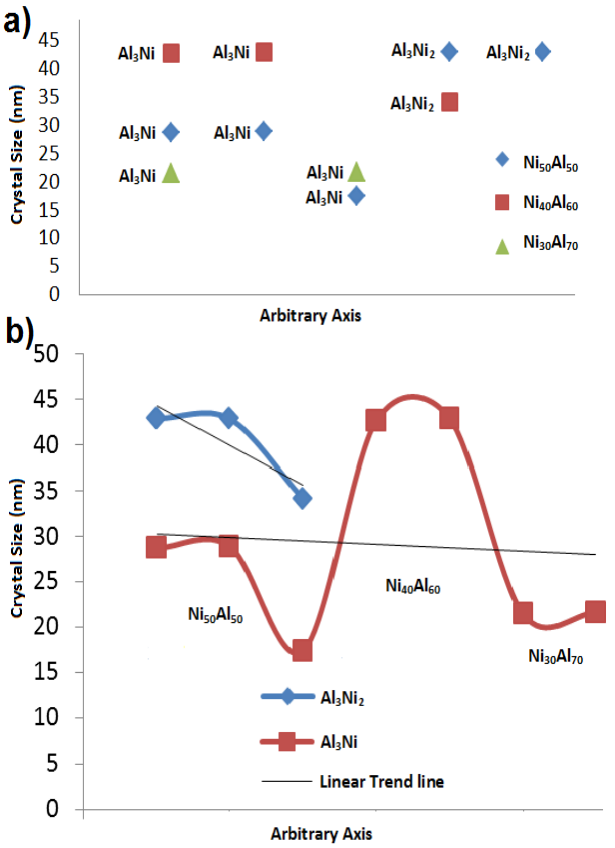

Fig. 3: a) Variation of crystal size of the alloys, and b) comparison of crystal size of the Al_3Ni and Al_3Ni_2.

From the EDX spectrum presented in Fig. 4, we can see that there are three basic types of peaks such as oxygen (O), Ni and Al after 5 h dealloying. Ni peaks formed at 0.84, 7.40, and 8.14 keV X-ray energy. O and Al spectrums have appeared corresponding to 0.24 keV and 1.50 keV X-ray energy, respectively. The presence of oxygen in EDX data ensures the oxide formation. It is assumed that that these oxide products were Al_2O_3 and NiO.

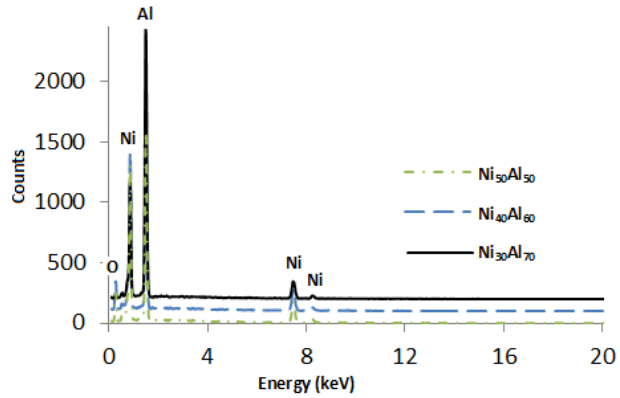

Fig. 4: EDX spectrums of nanoporous Ni obtained after 5 h dealloying

Figure 5 shows the SEM images of dealloyed Ni_xAl_{1-x} alloys. There were hardly any pores in nanoscale observed in the dealloyed $Ni_{50}Al_{50}$ and $Ni_{40}Al_{60}$ alloys. Although $Ni_{30}Al_{70}$ shows nanoporous structure, as shown in Fig. 5(c), a substantial amount of Al remains after dealloying which was proved by EDX spectrums as shown in Fig. 4, and EDX data in Table 2.

Table 2: EDX data for elemental analysis after 5 h dealloying

Alloy	Element	Weight %	Atomic %
$Ni_{50}Al_{50}$	Al	51.29	69.62
	Ni	48.71	30.38
$Ni_{40}Al_{60}$	O	3.79	7.79
	Al	58.08	70.83
	Ni	38.14	21.38
$Ni_{30}Al_{70}$	Al	67.02	81.55
	Ni	32.98	18.45

Moreover, it has been reported that the residual Al can not be removed but asymptotically reaches a limit at exhaustively long etching or dealloying time (up to 100 h) [24, 25]. It is known that the evolution of porous structure during dealloying involves etching of less noble (LN) element coupled with coarsening of more noble (MN) element by surface diffusion. Surface diffusion of MN element along alloy interfaces plays a key role in the formation of nanoporous metal [26].

It has been reported that the surface diffusivity $D_{(s)}$ of metal atoms can be given by the following equation:

$$D_{(s)}=[d_{(t)}]^4 kT/32\gamma ta^4 \quad (5)$$

Where k is Boltzmann constant (1.3806×10^{-23} J K^{-1}), t is the dealloying time, T is the dealloying temperature, γ is the surface energy (γ_{Ni}= 2.00 J m^{-2} [27]), $d_{(t)}$ is the ligament length, and a is lattice parameter ($a_{Ni}=3.5238\times10^{-10}$ m). The calculated $D_{(s)}$ at 60 ^oC for 5 h dealloying time is 2.7826×10^{-17} which is smaller than the reported by Qiu et. al [28]. The complete leaching out of Al was not observed. Therefore, the surface diffusivity of Ni can be improved by increasing the dealloying temperature, or by decreasing dealloying time. In contrast, high temperature also promotes Ni dissolution in strong alkali and leads to destruction of nanoporous Ni.

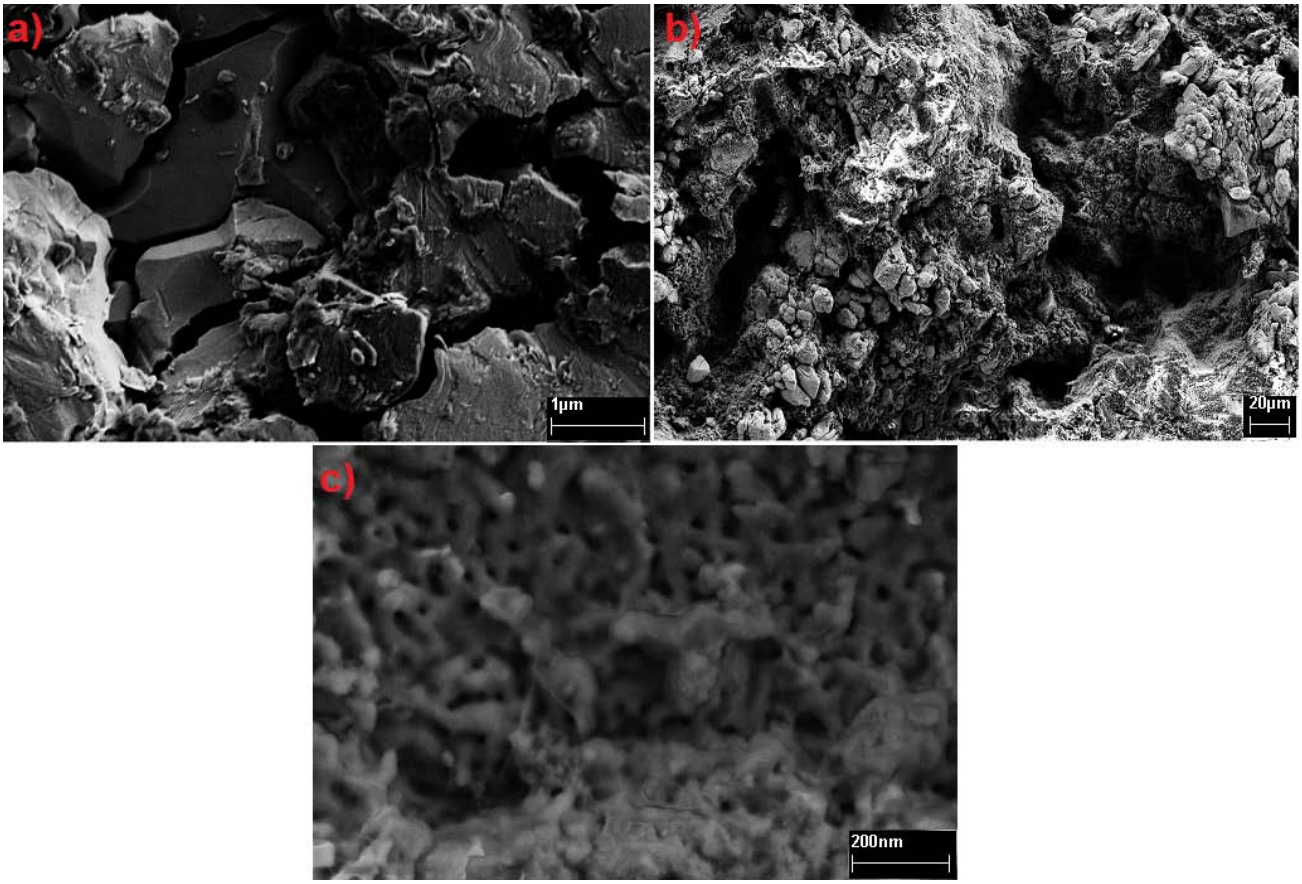

Fig. 5: SEM images of dealloyed Ni_xAl_{1-x} alloys: a) $Ni_{50}Al_{50}$, b) $Ni_{40}Al_{60}$, and c) $Ni_{30}Al_{70}$

5. CONCLUSIONS

The use of porous metals has generated much excitement in the field of energy storage and other fields. In this study, fabrication of nanoporous Ni foam was attempted by dealloying the aluminum from $Ni_{50}Al_{50}$, $Ni_{40}Al_{60}$, and $Ni_{30}Al_{70}$ alloys made by powder metallurgy. Nanoporous Ni structure was observed on the surface of $Ni_{30}Al_{70}$ alloy after dealloying in a handmade cell using a NaOH solution at 60 ^{o}C; whilst there was hardly any pore at nanoscale observed in the dealloyed $Ni_{50}Al_{50}$ and $Ni_{40}Al_{60}$ alloys. The pore and ligament size of the nanoporous Ni is approximately 40 and 100 nm, respectively. EDX data suggested that there was still residue aluminum remained in the nanoporous Ni foam.

6. ACKOWLEDGEMENT

This project is supported by the Australian Government through the Australia-India Strategic Research Fund (ST060048).

7. REFERENCES

1. Lefebvre, L.-P., J. Banhart, and D. Dunand, Porous metals and metallic foams: current status and recent developments. Advanced Engineering Materials, 2008. 10(9): p. 775-787.
2. Banhart, J., Manufacture, characterisation and application of cellular metals and metal foams. Progress in materials science, 2001. 46(6): p. 559-632.
3. Hooman, K., A. Tamayol, and M. Malayeri, Impact of Particulate Deposition on the Thermohydraulic Performance of Metal Foam Heat Exchangers: A Simplified Theoretical Model. Journal of Heat Transfer, 2012. 134: p. 092601.
4. Odabaee, M., et al., Particle deposition effects on heat transfer from a metal foam-wrapped tube bundle. International Journal of Numerical Methods for Heat & Fluid Flow, 2013. 23(1): p. 74-87.
5. Wen, C., et al., Processing of fine-grained aluminum foam by spark plasma sintering. Journal of materials science letters, 2003. 22(20): p. 1407-1409.
6. Ashby, M.F., et al., Metal Foams: A Design Guide: A Design Guide. 2000: Butterworth-Heinemann.
7. Hua, Z., et al., Low-density nanoporous iron foams synthesized by sol-gel autocombustion. Nanoscale research letters, 2012. **7**(1): p. 129.
8. Pierotti, R. and J. Rouquerol, Reporting physisorption data for gas/solid systems with special reference to the determination of surface area and porosity. Pure Appl Chem, 1985. **57**(4): p. 603-619.
9. Rouquerol, J., et al., Recommendations for the

characterization of porous solids (Technical Report). Pure and Applied Chemistry, 1994. **66**(8): p. 1739-1758.
10. Kennedy, A., Porous Metals and Metal Foams Made from Powders. Edited by Katsuyoshi Kondoh, 2012: p. 31.
11. Tappan, B.C., S.A. Steiner, and E.P. Luther, Nanoporous metal foams. Angewandte Chemie International Edition, 2010. 49(27): p. 4544-4565.
12. Raney, M., Method of producing finely-divided nickel. 1927, US patent 1,628,190.
13. Olurin, O.B., et al., Strength and ductility of as-plated and sintered CVD nickel foams. Composites Science and Technology, 2003. **63**(16): p. 2317-2329.
14. Paserin, V., et al., CVD technique for Inco nickel foam production. Advanced Engineering Materials, 2004. 6(6): p. 454-459.
15. Yamada, Y., et al. Preparation and characterisation of open-cell microporous nickel. in Materials science forum. 2007. Trans Tech Publ.
16. Marozzi, C.A. and A.C. Chialvo, Development of electrode morphologies of interest in electrocatalysis. Part 1: Electrodeposited porous nickel electrodes. Electrochimica Acta, 2000. 45(13): p. 2111-2120.
17. Hakamada, M. and M. Mabuchi, Preparation of nanoporous Ni and Ni–Cu by dealloying of rolled Ni–Mn and Ni–Cu–Mn alloys. Journal of Alloys and Compounds, 2009. 485(1–2): p. 583-587.
18. Sun, L., C.-L. Chien, and P.C. Searson, Fabrication of nanoporous nickel by electrochemical dealloying. Chemistry of materials, 2004. 16(16): p. 3125-3129.
19. Jiang, B., Z. Wang, and N. Zhao, Effect of pore size and relative density on the mechanical properties of open cell aluminum foams. Scripta Materialia, 2007. 56(2): p. 169-172.
20. Imwinkelried, T., Mechanical properties of open-pore titanium foam. Journal of Biomedical Materials Research Part A, 2007. **81**(4): p. 964-970.
21. Zhang, J. and C.M. Li, Nanoporous metals: fabrication strategies and advanced electrochemical applications in catalysis, sensing and energy systems. Chemical Society Reviews, 2012. 41(21): p. 7016-7031.
22. Pickering, H.W., Characteristic features of alloy polarization curves. Corrosion Science, 1983. **23**(10): p. 1107-1120.
23. Wagner, K., et al., Dealloying below the critical potential. Journal of the Electrochemical Society, 1997. 144(10): p. 3545-3555.
24. Wang, X., et al., Influence of Alloy Composition and Dealloying Solution on the Formation and Microstructure of Monolithic Nanoporous Silver through Chemical Dealloying of Al– Ag Alloys. The Journal of Physical Chemistry C, 2009. 113(30): p. 13139-13150.
25. Qi, Z., et al., Alloy composition dependence of formation of porous Ni prepared by rapid solidification and chemical dealloying. Journal of Alloys and Compounds, 2009. 472(1): p. 71-78.
26. Liu, W., et al., Influence of Dealloying Solution on the Microstructure of Monolithic Nanoporous Copper through Chemical Dealloying of Al 30 at.% Cu Alloy. Int. J. Electrochem. Sci, 2012. **7**: p. 7993-8006.
27. Tyson, W. and W. Miller, Surface free energies of solid metals: estimation from liquid surface tension measurements. Surface Science, 1977. 62(1): p. 267-276.
28. Qiu, H.-J., et al., Fabrication of large-scale nanoporous nickel with a tunable pore size for energy storage. Journal of Power Sources, 2013.